Chaotic resonance: Two-state model with chaos-induced escape over potential barrier

L. Y. Chew,[1] Christopher Ting,[3,2] and C. H. Lai[2]
[1]*School of Physical and Mathematical Sciences, Nanyang Technological University, Singapore 637616*
[2]*Department of Physics, National University of Singapore, Singapore 117542*
[3]*Singapore Management University, Singapore 259756*
(Received 13 October 2004; revised manuscript received 29 June 2005; published 30 September 2005)

We consider the resonant effects of chaotic fluctuations on a strongly damped particle in a bistable potential driven by weak sinusoidal perturbation. We derive analytical expressions of chaos-induced transition rate between the neighboring potential wells based on the inhomogeneous Smoluchowski equation. Our first-order analysis reveals that the transition rate has the form of the Kramers escape rate except for a perturbed prefactor. This modification to the prefactor is found to arise from the statistical asymmetry of the chaotic noise. By means of the two-state model and the chaos-induced transition rate, we arrive at an analytical expression of the signal-to-noise ratio (SNR). Our first-order SNR shows that chaotic resonance can correspond directly to stochastic resonance.

DOI: 10.1103/PhysRevE.72.036222 PACS number(s): 05.45.−a, 05.40.−a, 02.50.−r, 82.20.−w

I. INTRODUCTION

Stochastic resonance (SR) is the phenomenon where a weak periodic signal is enhanced through the cooperative effect of noise in a nonlinear system [1]. It is found in diverse fields such as physics [2], biology [3], and chemistry [4]. Although SR arises in stochastic systems, similar amplification is found to occur in deterministic systems in chaos, with the appearance of a maximum signal-to-noise ratio (SNR) at a certain chaotic noise strength. This dynamical resonant behavior, with the role of noise substituted by chaos, is termed "chaotic resonance" [5–7].

Chaotic resonance (CR)—according to various theoretical and experimental studies—can be produced in two ways: via intrinsic or extrinsic chaos [5,8]. In the former case, the chaos is inherent within the dynamical system which evolves in a regime near a crisis [9]. When the intermittent chaos-induced transition between two internal dynamic states becomes synchronized with an external weak periodic force, CR occurs. In the extrinsic case, chaos is supplied externally [5]. It replaces the stochastic noise of conventional SR. As the chaotic fluctuations induce, with the weak periodic forcing, coherent transitions between the bistable states in the same manner as stochastic noise, CR results. This latter scenario was verified by Ippen *et al.* [5] through the replacement of white Gaussian noise in their overdamped Duffing equation with Ulam map dynamics. Their numerical studies have uncovered that, within experimental error, CR and SR are equal.

In this paper, we develop further insights into the correspondence between SR and CR when the chaotic noise is added externally. We construct a two-state model of a chaotic kicked particle in a bistable potential along with a slow sinusoidal perturbation. We first determine the rate equation that gives the transition time scale between the two states when the particle is driven solely by chaotic noise [10]. The resulting analytical derivation of the Kramers escape rate for chaotic fluctuations is given in Sec. II. In Sec. III, we employ the theoretical approach of McNamara and Wiesenfeld [11] with the escape rate derived in Sec. II to investigate the phenomenon of CR through the characteristic quantity of SNR. We discuss the first-order SNR due to chaotic perturbation obtained in this section and make comparison with that of conventional SR. Section IV summarizes and concludes the paper.

II. CHAOS-INDUCED KRAMERS ESCAPE RATE

A. The chaotic kicked particle model

Consider a simple model of a Brownian particle in a potential $V(x)$ subjected to periodic impulsive kick F_n at a frequency of $1/\tau$, with n being the discrete time stamp. The particle is, in addition, being acted upon by a viscous force. Then, the phase space trajectory of the Brownian particle (p_n, x_n) can be described by the following quasistationary kicked particle (QKP) map in the strong friction regime [12]

$$F_{n+1} = G^{(N)}(F_n), \tag{1}$$

$$p_{n+1} = e^{-\gamma\tau} p_n - \frac{V'(x_n)}{\gamma}\psi + (\gamma\tau)^{1/2} s F_{n+1}, \tag{2}$$

$$x_{n+1} = x_n + \frac{\psi}{\gamma} p_n - \frac{V'(x_n)}{\gamma}\left(\tau - \frac{1}{\gamma}\psi\right), \tag{3}$$

where $\psi = 1 - e^{-\gamma\tau}$, and γ is the damping constant. The scaling factor s^2 is the intensity of the noise. We express it as $s^2 = 4kT$, with k being the Boltzmann constant and T the temperature. By taking the overdamped limit, the QKP map is simplified to the following form:

$$F_{n+1} = G^{(N)}(F_n), \tag{4}$$

$$x_{n+1} = x_n + \left(\frac{\tau}{\gamma}\right)^{1/2} s F_n - \left(\frac{\tau}{\gamma}\right) V'(x_n). \tag{5}$$

Note that the "heat" source $G^{(N)}$ is, specifically, the Tchebyscheff map of order N. The probability distribution function of these one-dimensional maps are known to be non-

Gaussian [13]. Employing $\langle\cdots\rangle$ to denote the expectation with respect to the invariant measure $h(\cdots)$ of the dynamics of $G^{(N)}$, we have for all i and j,

$$\langle F_j\rangle = 0; \quad \langle F_i F_j\rangle = \frac{1}{2}\delta_K(i,j), \tag{6}$$

where $\delta_K(\cdots)$ is the Kronecker delta function.

The interest in a heat source out of iterates of Tchebyscheff maps stems from its ergodic, mixing, and chaotic nature. A map of order N possesses a positive Lyapunov exponent of $\ln N$. By treating τ as a fluctuation time scale of the system, the Kolmogorov-Sinai entropy of the heat bath turns out to be $\ln N/\tau$, which approaches infinity as $\tau\to 0$, implying that a single fast chaotic degree of freedom is able to generate stochasticity [14]. In this context of vanishing time scale, Tchebyscheff maps dynamics is able to induce Brownian motion in the case of free field [15]. After all, determinism has not disappeared with the emergence of stochastic behavior. It has simply been relegated when the time scale is infinitesimally small. By increasing the interval τ between chaotic kicks, the predictability time scale of the system is raised and deterministic effects become more apparent [16]. The physical consequence of such a change in time scale is addressed by our discrete-time model, which captures the deterministic correlations in the chaotic fluctuations.

A mathematically convenient feature of fluctuations from Tchebyscheff maps is that all their correlation properties are known [17]:

$$\left\langle \prod_{i=1}^{r} F_{n_i} \right\rangle = \left(\frac{1}{2}\right)^r \sum_{\sigma} \delta_K\left(\sum_{i=1}^{r} \sigma_i N^{n_i}, 0\right), \tag{7}$$

where Σ_σ is the summation over all possible configurations $(\sigma_1,\ldots,\sigma_r)$, with $\sigma_i=\pm 1$. Note that Eq. (6) is a special case of Eq. (7) and the first two correlations correspond to those of white Gaussian noise. Although the higher-order correlations are different from the white Gaussian model, they are nonetheless close to it compared to those generated by other smooth chaotic systems. Furthermore, for this class of map, the odd-order correlations exist when N is even, but all vanish when N is odd [18]. Thus, fluctuations from the odd-order Tchebyscheff maps are said to be statistically symmetric, while those from the even-order Tchebyscheff maps are statistically asymmetric [19,20].

B. A reflective and symmetric potential field

We begin by assuming the following perturbative ansatz [21]:

$$\rho(F,x,t) = \rho^{(0)}(F,x,t) + \sum_{i=1}^{\infty} (\tau/\gamma)^{i/2} q^{(i)}(F,x,t), \tag{8}$$

such that $\rho^{(0)}$ is the zeroth-order probability density, while the $q^{(i)}$'s are the ith order correction terms. By means of the Perron-Frobenius approach, the behavior of an ensemble of particles given by Eqs. (4) and (5) satisfies the associated inhomogeneous Smoluchowski equation [12]

$$\frac{kT}{\gamma}\frac{\partial^2 P_1}{\partial x^2} + \frac{\partial}{\partial x}\left(\frac{V'(x)P_1}{\gamma}\right) - \frac{\partial P_1}{\partial t} = \tau^{1/2}\gamma^{-3/2}\frac{\partial}{\partial x}\int_{-1}^{1} dFsFq^{(2)}(F,x,t). \tag{9}$$

Note that τ/γ is the perturbative parameter, while $P_1(x,t)$ is the first-order position probability distribution. Also, Eq. (9) is applicable only to Tchebyscheff maps of even order, as $\rho^{(1)}$ is separable in this case $\rho^{(1)}=h(F)P_1(x,t)$, with

$$P_1(x,t) = P_0(x,t) + (\tau/\gamma)^{1/2} Q_1(x,t). \tag{10}$$

Equation (9) can also be reexpressed in the form of a first-order differential equation

$$\frac{kT}{\gamma}\frac{\partial P_1}{\partial x} + \frac{V'(x)}{\gamma}P_1 = \tau^{1/2}\gamma^{-3/2}\int_{-1}^{1} dFsFq^{(2)} - \mathcal{J}_1, \tag{11}$$

where $\mathcal{J}_1$ is the first-order probability current by virtue of the following relation:

$$\frac{\partial P_1}{\partial t} = -\frac{\partial \mathcal{J}_1}{\partial x}, \tag{12}$$

which describes probability conservation. Because $\partial P_1/\partial t = 0$ in the steady state, we expect the probability current $\mathcal{J}_1$ to be a constant asymptotically.

Let us first consider a potential field $V(x)$ that possesses the characteristic of spatial symmetry as well as positive spatial divergence as $x\to\pm\infty$. With $V(x)\to\infty$ as $x\to\pm\infty$, the probability P_1 and the probability current $\mathcal{J}_1$ must vanish at these points. In other words, the boundaries at $x\to\pm\infty$ are considered to be reflective [22]. At equilibrium, we also expect $\mathcal{J}_1$ to vanish everywhere. These conditions lead to the following simplification:

$$\frac{kT}{\gamma}\frac{\partial P_1}{\partial x} + \frac{V'(x)}{\gamma}P_1 = \tau^{1/2}\gamma^{-3/2}\int_{-1}^{1} dFsFq^{(2)}, \tag{13}$$

whose solution is given by

$$P_1(x) = N_1 e^{-V(x)/kT} + \left(\frac{\tau}{\gamma}\right)^{1/2}\frac{1}{kT}e^{-V(x)/kT}\Phi(x). \tag{14}$$

N_1 is the constant of integration. We have also simplified the notation by writing

$$\Phi(x) = \int_{-\infty}^{x} e^{V(x')/kT}\int_{-1}^{1} dFsFq^{(2)}(F,x')dx'. \tag{15}$$

The normalization of $P_1(x)$ then implies

$$N_1 = \frac{1}{Z}\left\{1 - \left(\frac{\tau}{\gamma}\right)^{1/2}\frac{1}{kT}\int_{-\infty}^{\infty} e^{-V(x')/kT}\Phi(x')dx'\right\}, \tag{16}$$

with

$$Z = \int_{-\infty}^{\infty} e^{-V(x)/kT}dx. \tag{17}$$

Thus,

$$P_1(x) = \frac{1}{Z}e^{-V(x)/kT} + \left(\frac{\tau}{\gamma}\right)^{1/2}\frac{1}{kT}e^{-V(x)/kT} \times\left\{\Phi(x) - \frac{1}{Z}\int_{-\infty}^{\infty} e^{-V(x')/kT}\Phi(x')dx'\right\}. \quad (18)$$

Note that the first term on the right-hand side of Eq. (18) is $P_0(x)$, while the second term is $(\tau/\gamma)^{1/2}Q_1(x)$, which is the first-order correction due to the asymmetric chaotic fluctuations.

We would like to indicate that the inhomogeneous term $\int_{-1}^{1} dFsFq^{(2)}(F,x)$ has been calculated explicitly only for chaotic fluctuations from the $G^{(2)}$ map [12]. The outcome is

$$\int_{-1}^{1} dFsFq^{(2)}(F,x) = \frac{(kT)^{1/2}}{Z}e^{-V(x)/kT}\left[\frac{V'(x)^2}{kT} - V''(x)\right]. \quad (19)$$

Putting Eq. (19) into Eq. (15), we have

$$\Phi(x) = \frac{(kT)^{1/2}}{Z}\int_{-\infty}^{x}\left[\frac{V'(x')^2}{kT} - V''(x')\right]dx'. \quad (20)$$

Interestingly, $\Phi(x)$ is antisymmetric in this case when the potential is symmetric, with the consequence that

$$\int_{-\infty}^{\infty} e^{-V(x)/kT}\Phi(x)dx = 0 \quad (21)$$

for the $G^{(2)}$ map fluctuations.

C. A harmonic potential

The harmonic potential

$$V_h(x) = \frac{1}{2}\omega x^2 \quad (22)$$

is a symmetric and reflective potential, and is of interest to the chaos-induced transition rate problem to be discussed in the next subsection. For the harmonic potential, the first-order probability distribution of the particle in the well kicked by fluctuations from even-order Tchebyscheff maps is

$$P_1(x) = \left\{\sqrt{\frac{\omega}{2\pi kT}} + \left(\frac{\tau}{\gamma}\right)^{1/2}\frac{1}{kT}\left[\Phi(x) - \sqrt{\frac{\omega}{2\pi kT}} \times\int_{-\infty}^{\infty} e^{-\omega x'^2/2kT}\Phi(x')dx'\right]\right\}e^{-\omega x^2/2kT}, \quad (23)$$

as

$$Z = \int_{-\infty}^{\infty} e^{-\omega x^2/2kT}dx = \sqrt{\frac{2\pi kT}{\omega}} \quad (24)$$

or

$$P_1(0) = \sqrt{\omega/2\pi kT}. \quad (25)$$

Consequently, the ensemble of particles, instead of thermalizing to the usual Maxwell-Boltzmann distribution, settles down to a perturbatively modified version within the harmonic potential well.

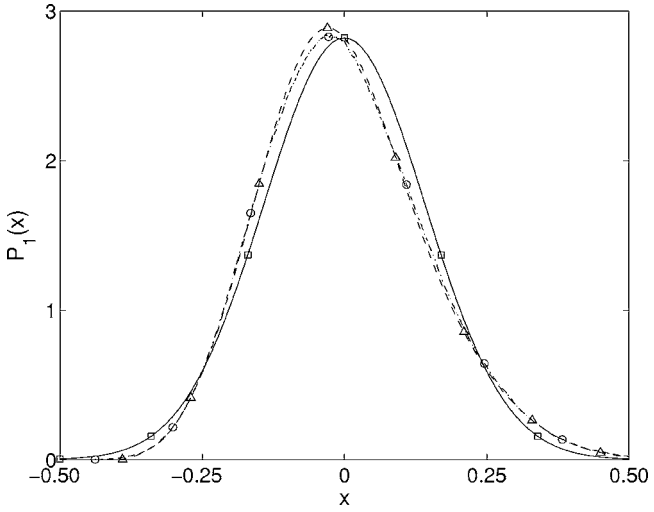

FIG. 1. The first-order probability distribution function of the particle in a harmonic potential based on analytical expression Eq. (27) (dashed curve with triangle markers) and numerical simulation (dashed-dotted curve with circle markers) for chaotic fluctuations from the $G^{(2)}$ map. The Maxwell-Boltzmann distribution is represented by the solid curve with square markers. The parameters in dimensionless units are $m=1.0$, $\tau=1.0$, $\gamma=200.0$, $kT=0.2$, $\omega=10.0$. The ensemble size used in the numerical simulation is 1×10^5, with an iteration length of 2×10^3.

In particular, if the chaotic fluctuation is from the $G^{(2)}$ map, we have

$$\Phi(x) = \frac{(kT)^{1/2}}{Z}\left(\frac{\omega^2x^3}{3kT} - \omega x\right) \quad (26)$$

and

$$P_1(x) = \left[1 + \left(\frac{\tau}{\gamma kT}\right)^{1/2}\left(\frac{\omega^2}{3kT}x^3 - \omega x\right)\right]\sqrt{\frac{\omega}{2\pi kT}}e^{-\omega x^2/2kT}. \quad (27)$$

This analytical result is plotted in Fig. 1, which shows close correspondence with that obtained from numerical simulation. Comparing them against the Maxwell-Boltzmann distribution

$$P(x) = \sqrt{\frac{\omega}{2\pi kT}}e^{-\omega x^2/2kT}, \quad (28)$$

we observe that the statistical asymmetry of the fluctuation results in a desymmetrization of the probability distribution. This desymmetrization of the probability distribution is expected to dimish, however, for $G^{(4)}$ map fluctuation, because the correction factor scales in the order of $(\tau/\gamma)^{3/2}$ in this case [12], instead of $(\tau/\gamma)^{1/2}$ for $G^{(2)}$ map fluctuation. Through numerical simulation (see Fig. 2), we see that the desymmetrization reduces so fast that the probability distribution is found to closely match the Maxwell-Boltzmann distribution. Next, let us examine the effect of fluctuation from $G^{(3)}$ map. As a result of its statistical symmetry and the

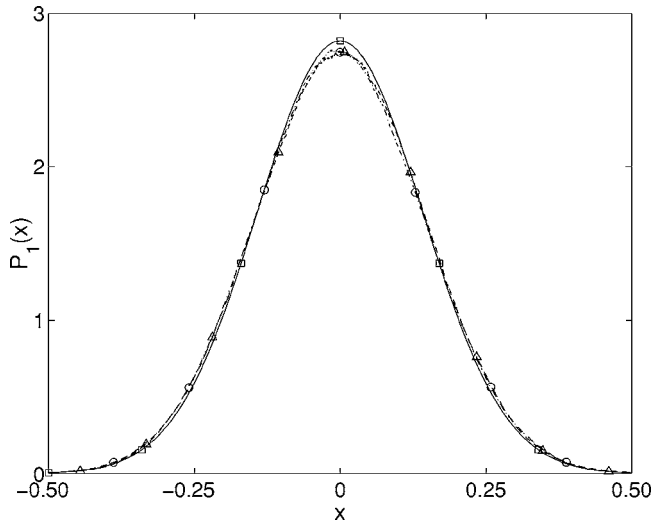

FIG. 2. The first-order probability distribution function of the particle in a harmonic potential based on numerical simulations for chaotic fluctuations from $G^{(3)}$ (dashed-dotted curve with circle markers) and $G^{(4)}$ (dashed curve with triangle markers) maps. The Maxwell-Boltzmann distribution is represented by the solid curve with square markers. The parameters in dimensionless units are $m=1.0$, $\tau=1.0$, $\gamma=200.0$, $kT=0.2$, $\omega=10.0$. The ensemble size used in the numerical simulation is 1×10^5, with an iteration length of 2×10^3.

symmetry of the harmonic potential, we anticipate the probability distribution of the particle driven by its dynamics to be symmetric. This is indeed confirmed through numerical simulation as in Fig. 2. More significantly, the distribution is found to agree remarkably well with the Maxwell-Boltzmann distribution.

Finally, with the fluctuations F_i being restricted within the range $[-1,1]$, the stationary probability density [Eq. (18)] is expected to possess a bounded support for a confining potential when τ, γ, and T are finite [23]. However, it is observed that $P_0(x)$, being the solution to the leading order Smoluchowski equation, has unbounded support. Such convergence towards a stationary probability density with unbounded support in the zeroth-order limit can be understood by considering the harmonic potential. Applying Eq. (5) to the harmonic potential, we obtain for large n,

$$x_{n+1}=\sum_{i=0}^{n}X_i=s\left(\frac{\tau}{\gamma}\right)^{1/2}\sum_{i=0}^{n}\left[1-\left(\frac{\tau}{\gamma}\right)\omega\right]^{n-i}F_i, \tag{29}$$

with $0<[1-(\tau/\gamma)\omega]<1$. Note that $X_i=s(\tau/\gamma)^{1/2}[1-(\tau/\gamma)\omega]^{n-i}F_i$. The variance of x_{n+1} is then found to be

$$\lim_{n\to\infty}\langle x_{n+1}^2\rangle=\left(\frac{\tau}{\gamma}\right)\frac{s^2/2}{1-[1-(\tau/\gamma)\omega]^2}, \tag{30}$$

which is a finite quantity. The maximum variance of X_i occurs when $i=n$, whose value is given by $\langle X_n^2\rangle=(\tau/\gamma)(s^2/2)$. The relative strength between $\langle X_n^2\rangle$ and $\langle x_{n+1}^2\rangle$ is given by β as follows:

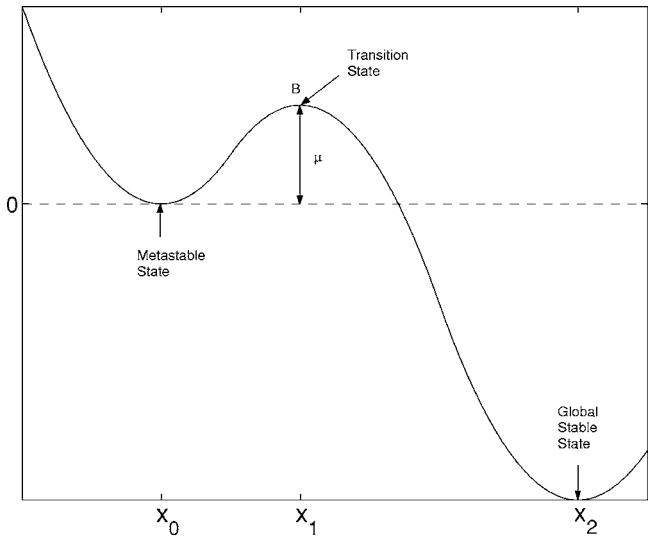

FIG. 3. The asymmetric potential of the Kramers problem.

$$\beta=\lim_{n\to\infty}\frac{\langle X_n^2\rangle}{\langle x_{n+1}^2\rangle}=\left(\frac{\tau}{\gamma}\right)\left[2\omega-\left(\frac{\tau}{\gamma}\right)\omega^2\right]. \tag{31}$$

In the limit $\tau/\gamma\to0$, β tends to 0, showing that the individual variances $\langle X_i^2\rangle$ are very small compared to their sum $\langle x_{n+1}^2\rangle$. In other words, for a given $\varepsilon>0$, $\langle X_i^2\rangle/\langle x_{n+1}^2\rangle<\varepsilon$ for all $i=1,\ldots,n$. This implies the satisfaction of the Lindeberg condition [24], and indicates the convergence of x_{n+1} to the normal distribution in the zeroth-order limit as expected from our first-order perturbation theory.

D. The transition rate over a potential barrier

The studies on thermally activated escape from metastable states or the rate of transition of a particle over a potential barrier are known as the Kramers problem. Kramers, in his pioneering work [25], derived the escape rate of such a particle in a potential well interacting with a heat bath of equilibrium fluctuations. The escape rate was found to have the form of an Arrhenius equation, but with a prefactor that depends on whether the interaction is moderately to strongly coupled (strong friction regime) or weakly coupled (weak friction regime) to the heat bath. In this subsection, we further explore the Kramers problem when the heat bath is generated by a class of chaotic nonequilibrium fluctuations. We derive the particle escape rate, including both the prefactor and the exponent. This theoretical result is essential in the analysis of CR in the next section.

Recall that the Kramers problem is concerned with the escape of particles from an asymmetric potential as shown in Fig. 3. This potential consists of two wells. The upper well (at x_0) is known as the metastable state, while the lower well (at x_2) is the global stable state. The top of the barrier that separates these two wells (indicated as B at x_1) is called the transition state. Note that we have adopted the convention $x_0=0$ and

$$V(x_0)=V(0)=0 \tag{32}$$

in the following analysis. Kramers problem can be viewed from the perspective of a boundary that is approximately

absorbing beyond the transition state [26], i.e.,

$$P_1(x) \approx 0 \quad \text{for } x > x_1, \tag{33}$$

with the escaped particle being removed by sinks after crossing the barrier.

Let us assume that the metastable state of the potential $V(x)$ is occupied by an ensemble of strongly damped particles. With our interest in chaotic fluctuations in the limit $\tau/\gamma \to 0$, it is sufficient to consider the probability density up till the first order in τ/γ. By restricting to the statistically asymmetric Tchebyscheff maps of even order, the position probability distribution $P_1(x,t)$ of the ensemble of particles satisfies the inhomogeneous Smoluchowski equation (9). This equation can be rewritten in the following way:

$$\frac{\partial P_1}{\partial t} = -\frac{\partial}{\partial x}\left[\tau^{1/2}\gamma^{-3/2}\int_{-1}^{1} dFsFq^{(2)}(F,x) - \frac{kT}{\gamma}\frac{\partial P_1}{\partial x} - \frac{V'(x)}{\gamma}P_1\right], \tag{34}$$

which allows us to again identify the probability current $\mathcal{J}_1$ [see Eq. (12)] as follows:

$$\mathcal{J}_1 = \tau^{1/2}\gamma^{-3/2}\int_{-1}^{1} dFsFq^{(2)}(F,x) - \frac{kT}{\gamma}\frac{\partial P_1}{\partial x} - \frac{V'(x)}{\gamma}P_1. \tag{35}$$

Considering the stationary situation in which the current is maintained by sources that supply the potential well with particles having energies of the order kT, while being absorbed by sinks beyond the transition state [26], $\mathcal{J}_1$ is constant and nonvanishing. In order to solve for $\mathcal{J}_1$, let us rewrite Eq. (35) in the following way:

$$\frac{\partial P_1}{\partial x} + \frac{V'(x)}{kT}P_1 = \left(\frac{\tau}{\gamma}\right)^{1/2}\frac{1}{kT}\int_{-1}^{1} dFsFq^{(2)}(F,x) - \frac{\gamma\mathcal{J}_1}{kT}, \tag{36}$$

which can be reduced to

$$\frac{\partial}{\partial x}\left(e^{V(x)/kT}P_1\right) = \left(\frac{\tau}{\gamma}\right)^{1/2}\frac{1}{kT}e^{V(x)/kT}\int_{-1}^{1} dFsFq^{(2)}(F,x) - \frac{\gamma\mathcal{J}_1}{kT}e^{V(x)/kT}. \tag{37}$$

Integrating Eq. (37) from x_0 to x_1^+, where $x_1^+ = x_1 + 0^+$ with 0^+ an infinitesimal quantity, we obtain

$$\left[e^{V(x)/kT}P_1\right]_{x_0}^{x_1^+} = \left(\frac{\tau}{\gamma}\right)^{1/2}\frac{1}{kT}\int_{x_0}^{x_1^+} e^{V(x)/kT}\int_{-1}^{1} dFsFq^{(2)}(F,x)dx - \frac{\gamma\mathcal{J}_1}{kT}\int_{x_0}^{x_1^+} e^{V(x)/kT}dx. \tag{38}$$

After a rearrangement and employing the conditions given by Eqs. (32) and (33), we have

$$\mathcal{J}_1 = \frac{kT}{\gamma}\frac{P_1(0)}{\int_{x_0}^{x_1^+} e^{V(x)/kT}dx} + \frac{\tau^{1/2}\gamma^{-3/2}\int_{x_0}^{x_1^+} e^{V(x)/kT}\int_{-1}^{1} dFsFq^{(2)}(F,x)dx}{\int_{x_0}^{x_1^+} e^{V(x)/kT}dx}. \tag{39}$$

We observed that the probability current $\mathcal{J}_1$ is influenced by the inhomogeneous term $\int_{-1}^{1} dFsFq^{(2)}(F,x)$, in addition to the first term on the right of Eq. (39) which appears in the Kramers treatment of the rate.

Given that the height of the potential barrier μ is large compared with the intensity of the chaotic noise kT, the particles will equilibrate in the neighborhood of the potential minimum at x_0, according to the "perturbed" Maxwell-Boltzmann distribution in Eq. (23). This ensues from adopting Kramers' assumption [25,27] that $V(x)$ is dominated by the parabolic part $\omega x^2/2$ at the metastable state. This assumption also applies to the transition state at x_1.

The escape rate, following Kramers, is given by

$$K_r = \frac{\mathcal{J}_1}{n_0}. \tag{40}$$

$\mathcal{J}_1$ is the probability current in Eq. (35), while

$$n_0 = \int_{x_0-\varepsilon}^{x_0+\varepsilon} P_1(x)dx, \tag{41}$$

where ε is a small number. When $\mu \gg kT$, n_0 is well approximated by

$$n_0 \approx \int_{-\infty}^{\infty} P_1(x)dx = 1. \tag{42}$$

As a result, K_r depends essentially on $\mathcal{J}_1$. It follows that

$$K_r = \frac{1}{\int_{x_0}^{x_1^+} e^{V(x)/kT}dx}\left[\frac{kT}{\gamma}P_1(0) + \tau^{1/2}\gamma^{-3/2} \times \int_{x_0}^{x_1^+} e^{V(x)/kT}\int_{-1}^{1} dFsFq^{(2)}(F,x)dx\right]. \tag{43}$$

In view of $\mu \gg kT$,

$$\int_{x_0}^{x_1^+} e^{V(x)/kT}dx \approx e^{\mu/kT}\int_{-\infty}^{\infty} e^{-\omega(x-x_1)^2/2kT}dx \approx e^{\mu/kT}\sqrt{\frac{2\pi kT}{\omega}}. \tag{44}$$

With $P_1(0) = \sqrt{\omega/(2\pi kT)}$ from Eq. (25), the escape rate due to chaotic fluctuating forces from even-order Tchebyscheff maps is given by

$$K_r = \left\{ 1 + \left(\frac{\tau}{\gamma}\right)^{1/2} \sqrt{\frac{2\pi}{\omega kT}} \int_{x_0}^{x_1^+} e^{V(x)/kT} \int_{-1}^{1} dFsF \times q^{(2)}(F,x)dx \right\} \frac{\omega}{2\pi\gamma} e^{-\mu/kT}. \quad (45)$$

Equation (45) is the central result of this section. It shows that the escape rate preserves the Arrhenius form even though the source of fluctuations is chaotic and non-Brownian, in contrast to escape rates due to other chaotic noise [23]. Although this is only true for perturbatively small τ/γ, it is rather surprising as the noise is intrinsically deterministic. Furthermore, when $\tau/\gamma \to 0$, the prefactor of K_r approaches one, indicating a convergence to the Kramers escape rate in the strong friction regime.

To illustrate our result, we select the second-order Tchebyscheff map as our fluctuating force. Let us first deduce how the quantity $\int_{-1}^{1} dFsFq^{(2)}(F,x)$ is being influenced by the imposed probability current under this circumstance. In Ref. [12], we have shown that $\int_{-1}^{1} dFsFq^{(2)}(F,x)$ is related to the zeroth-order probability distribution $P_0(x)$ in the following way:

$$\int_{-1}^{1} dFsFq^{(2)}(F,x) = (kT)^{3/2} \frac{\partial^2 P_0}{\partial x^2}. \quad (46)$$

Hence, $\int_{-1}^{1} dFsFq^{(2)}(F,x)$ is associated with the constant zeroth-order probability current $\mathcal{J}_0$, which is determined from the Smoluchowski equation [12]

$$\mathcal{J}_0 = -\frac{kT}{\gamma}\frac{\partial P_0}{\partial x} - \frac{V'(x)}{\gamma} P_0. \quad (47)$$

Solving for $P_0(x)$ from Eq. (47), we obtain [26]

$$P_0(x) = \frac{\gamma J_0}{kT} e^{-V(x)/kT} \int_{x}^{x_1^+} e^{V(x')/kT} dx'. \quad (48)$$

This solution satisfies the boundary condition for sources and sinks: when $x = x_1^+$, $P_0(x_1^+) = 0$; and when $x \sim x_0$, $P_0(x) = \sqrt{\omega/2\pi kT}\exp(-\omega x^2/2kT)$. Then, employing Eq. (46), we attain

$$\int_{-1}^{1} dFsFq^{(2)}(F,x) = \left\{ \left[\frac{V'(x)^2}{kT} - V''(x) \right] e^{-V(x)/kT} \times \int_{x}^{x_1^+} e^{V(x')/kT} dx' + V'(x) \right\} \frac{\gamma \mathcal{J}_0}{(kT)^{1/2}}. \quad (49)$$

Equation (49) shows the manner in which $\int_{-1}^{1} dFsF \times q^{(2)}(F,x)$ is being influenced by the introduction of sources and sinks.

Subsequently, by making use of the fact that $\mathcal{J}_0 = (\omega/2\pi\gamma)\exp(-\mu/kT)$ and the condition $\mu \gg kT$ such that the intensity of the chaotic noise is weak, we arrive at the following result:

$$\int_{x_0}^{x_1^+} e^{V(x)/kT} \int_{-1}^{1} dFsFq^{(2)}(F,x)dx = \sqrt{\frac{\omega}{2\pi}} \int_{x_0}^{x_1} \left[\frac{V'(x)^2}{kT} - V''(x) \right] dx, \quad (50)$$

where we have employed the fact that integrating from x_0 to x_1^+ is approximately the same as that from x_0 to x_1. In lieu of Kramers' parabolic approximations, we consider the potential

$$V_p(x) = \begin{cases} \frac{1}{2}\omega x^2 & \text{for } x \leqslant 0.5, \\ \mu - \frac{1}{2}\omega(x-1)^2 & \text{for } x > 0.5. \end{cases} \quad (51)$$

We have further restricted $\omega = 4\mu$ such that as μ increases, the transition state is maintained at $x_1 = 1$ while the two parabolic curves are continuously connected. These conditions result in

$$\int_{0}^{1} e^{V_p(x)/kT} \int_{-1}^{1} dFsFq^{(2)}(F,x)dx = \frac{\omega^{5/2}}{12kT\sqrt{2\pi}}. \quad (52)$$

Thus, for the $G^{(2)}$ map, the escape rate is of the following explicit form

$$K_r = \left\{ 1 + \frac{4}{3}\left(\frac{\tau}{\gamma}\right)^{1/2} \frac{\mu^2}{(kT)^{3/2}} \right\} \frac{\omega}{2\pi\gamma} e^{-\mu/kT}. \quad (53)$$

Note that the additional term $B = (4/3)(\tau/\gamma)^{1/2}[\mu^2/(kT)^{3/2}]$ in the prefactor is greater than zero. Hence, the deterministic $G^{(2)}$ chaotic noise has the effect of enhancing the rate of particle escape over the conventional Kramers rate, unlike results from other colored noise models, which typically show an escape rate suppression [23,26]. Furthermore, due to the bounded support of the stationary probability density at the metastable state, the escape rate will vanish below a critical threshold. In order for Eq. (53) to hold, we expect the threshold condition $kT > 2(\tau/\gamma)\mu^2$ to apply, according to estimates based on the adiabatic approximation [23].

From a qualitative perspective, the enhancement of the Kramers escape rate can be understood to arise from the statistical asymmetry of the noise. In the context of white Gaussian noise (which is statistically symmetric), classical theory predicts a quick thermalization of the ensemble of particles to the Maxwell-Boltzmann distribution in the well, while the nonequilibrium condition creates a diffusion current over the transition state. In the case of chaotic fluctuations due to even-order Tchebyscheff maps, thermalization also takes place, albeit with a Maxwell-Boltzmann distribution that is perturbed by a correction term. The consequent asymmetry in the distribution, as apparent from Eq. (23), depends on the magnitude of τ/γ, the form of the potential, and the noise intensity. By increasing τ, deterministic correlations become dominant. The consequence is a progressive desymmetrization of the distribution, which leads to an increase in activation rate beyond the standard Kramers rate.

This interesting feature is clearly depicted in Fig. 4, where numerical results are shown to closely match the theoretical

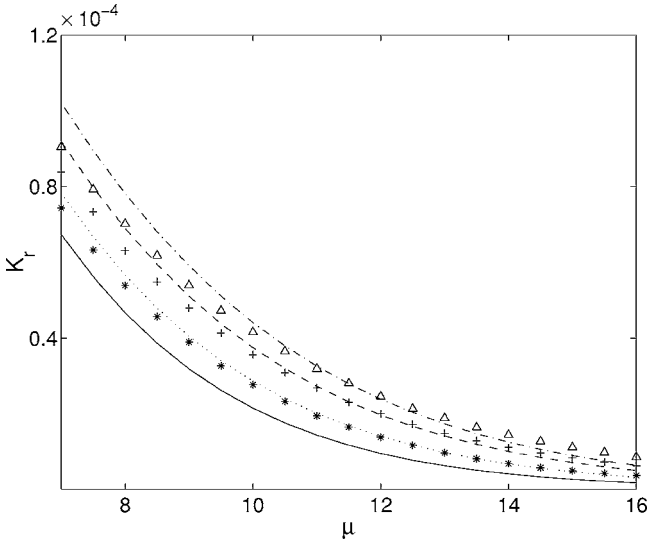

FIG. 4. The escape rate vs μ for $G^{(2)}$ map chaotic fluctuations with potential given by Eq. (51) based on analytical expression (53) (dashed-dotted, dashed, and dotted curves correspond to $\tau=1.0$, $\tau=0.5$, and $\tau=0.1$, respectively) and numerical simulation ($\triangle$, +, and * markers correspond to $\tau=1.0$, $\tau=0.5$, and $\tau=0.1$, respectively). Kramers' rate $K_r=(\omega/2\pi\gamma)\exp(-\mu/kT)$ is given by the solid curve. The parameters employed are $\gamma=2\times10^3$, $kT=2.0$. An ensemble size of 1×10^5 is used for the numerical simulations.

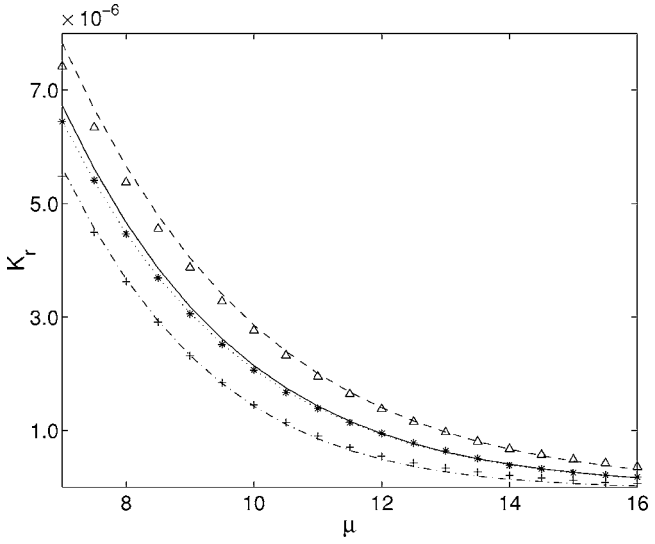

FIG. 5. The escape rate vs μ for different chaotic fluctuations: $G^{(2)}$ map (dashed curve—analytical expression; $\triangle$ markers—numerical simulation), Ulam map (dashed-dotted curve—analytical expression; + markers—numerical simulation), $G^{(3)}$ map (dotted curve—numerical simulation), and $G^{(4)}$ map (* markers—numerical simulation). Kramers' rate is given by the solid curve. The parameters employed are $\tau=1.0$, $\gamma=2\times10^4$, $kT=2.0$. An ensemble size of 1×10^5 is used for the numerical simulations.

outcomes, especially when $\tau/\gamma\to0$. Note that the escape rate from numerical simulations is obtained from the QKP map, with $K_r=(2t_{\mathrm{MFPT}})^{-1}$, where t_{MFPT} is the mean first-passage time [26]. In addition, the direction in which the Maxwell-Boltzmann distribution is desymmetrized depends on the sign of the odd-order correlations. For example, by using the Ulam map, which possesses odd-order correlations of opposite sign to those of the $G^{(2)}$ map, the distribution is desymmetrized in the opposite direction. The overall effect is a suppression of the escape rate given by

$$K_r=(1-B)\frac{\omega}{2\pi\gamma}e^{-\mu/kT}, \tag{54}$$

with $\tau/\gamma<9(kT)^3/(16\mu^4)$ (see Fig. 5). Thus, depending on the direction of desymmetrization, the Kramers escape rate is enhanced or suppressed accordingly. Such statistical asymmetric effects may be experimentally validated by optically trapping dielectric glass beads in a turbulent environment [28].

Interestingly, although statistical asymmetry has led to a deviation from Kramers rate, Eq. (45) shows that K_r converges to the Kramers escape rate for the class of even-order Tchebyscheff maps in the limit $\tau/\gamma\to0$, as the particle distribution in the well converges to the Maxwell-Boltzmann distribution. However, the rate of convergence to the "symmetric state"—the Kramers escape rate, can be different for a different even-order Tchebyscheff map. For the $G^{(2)}$ map, the convergence rate scales as $(\tau/\gamma)^{1/2}$, while for the $G^{(4)}$ map, we expect a more rapid rate of $O((\tau/\gamma)^{3/2})$ [12].

On the other hand, systems given by Eq. (51) with chaotic force from the class of odd-order Tchebyscheff maps can be considered as "symmetric." This is because these maps are statistically symmetric, and the potential $V(x)$ appears symmetric to the ensemble of particles if $\mu\gg kT$ and τ/γ is small. Consequently, no desymmetrization occurs, and we anticipate the escape rate to be the Kramers rate. Indeed, this is verified numerically for the case of the $G^{(3)}$ map (refer to Fig. 5).

In a nutshell, we have found that the odd higher-order correlations in the chaotic fluctuation are pivotal in either enhancing or suppressing the particle's activation over a potential barrier. The implication is that statistical asymmetry provides a mechanism to either speed up or slow down a particular reaction. This mechanism can also be used to control the transfer rate of particles within intricate Brownian ratchet devices.

III. THEORETICAL ANALYSIS OF CHAOTIC RESONANCE

A. A bistable potential

An essential ingredient for SR (or CR) consists of a bistable potential, such as the symmetric and reflective quartic potential as follows:

$$V_d(x)=-\frac{1}{2}x^2+\frac{1}{4}x^4. \tag{55}$$

Let us first ignore the presence of the weak periodic perturbation, and consider a strongly damped particle in the quartic potential being acted by chaotic forces that follow the dynamics of even-order Tchebyscheff maps [29]. The first-order probability distribution of this particle will equilibrate

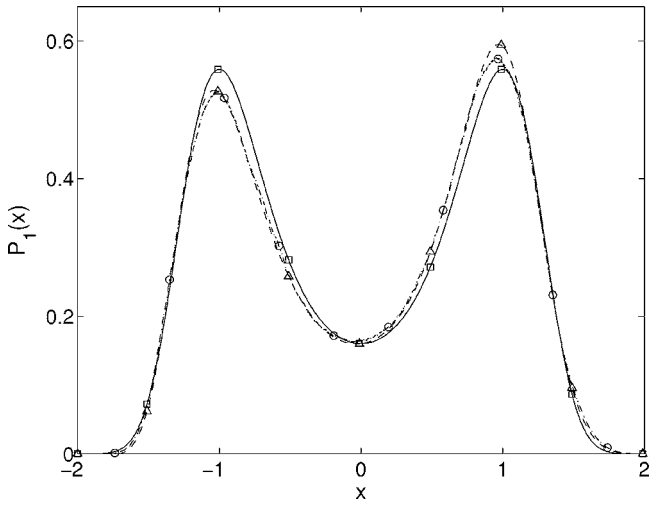

FIG. 6. The first-order probability distribution function of the particle in a bistable potential based on analytical expression (56) (dashed curve with triangle markers) and numerical simulation (dashed-dotted curve with circle markers) for chaotic fluctuations from $G^{(2)}$ map. The unperturbed distribution is represented by the solid curve with square markers. The parameters in dimensionless units are: $m=1.0$, $\tau=1.0$, $\gamma=200.0$, $kT=0.2$. The ensemble size used in the numerical simulation is 1×10^5, with an iteration length of 5×10^3.

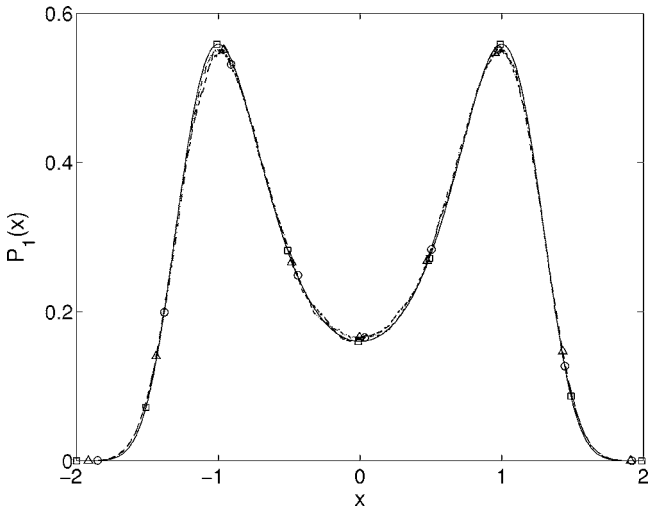

FIG. 7. The first-order probability distribution function of the particle in a bistable potential based on numerical simulations for chaotic fluctuations from $G^{(3)}$ (dashed-dotted curve with circle markers) and $G^{(4)}$ (dashed curve with triangle markers) maps. The unperturbed distribution is represented by the solid curve with square markers. The parameters in dimensionless units are $m=1.0$, $\tau=1.0$, $\gamma=200.0$, $kT=0.2$. The ensemble size used in the numerical simulation is 1×10^5, with an iteration length of 5×10^3.

to Eq. (18) with $V(x)$ replaced by $V_d(x)$. Furthermore, if the fluctuation arises from the $G^{(2)}$ map, this first-order distribution is further reducible to the following form:

$$P_1(x)=\left\{1+\left(\frac{\tau}{\gamma kT}\right)^{1/2}\left[\frac{1}{7kT}x^7-\frac{2}{5kT}x^5+\left(\frac{1}{3kT}-1\right)x^3+x\right]\right\}\frac{1}{Z}e^{-V_d(x)/kT}. \tag{56}$$

This analytical result and the corresponding outcome from simulation based on the QKP map is shown in Fig. 6, while Fig. 7 illustrates simulation results for fluctuations based on the $G^{(3)}$ and $G^{(4)}$ maps. Analogous to the harmonic potential, the probability distibution is found to desymmetrize in the case of the $G^{(2)}$ map. It converges more quickly to the unperturbed distribution $\exp[-V_d(x)/kT]/Z$ for the $G^{(4)}$ map. Finally, the distribution from the $G^{(3)}$ map is also observed to be consistent with the symmetric unperturbed distribution.

B. Chaotic kicked particle model with sinusoidal force of slow variation

Next, let us include a slow sinusoidal force $A_0\cos(\Omega t+\varphi)$ to our chaotic kicked particle model. The degree of slowness is captured by the frequency Ω (see Appendix A). We shall make two assumptions with regards to Ω. The first assumption is that the period of the sinusoidal perturbation $\mathcal{T}$ is much larger than the period of the kick, i.e., $\mathcal{T}=2\pi/\Omega \gg \tau$. More specifically, we require

$$\Omega\tau \ll 1. \tag{57}$$

For the second assumption, we consider the relaxation rate of the particle after the kick (or the dissipation rate) to be much shorter than the period of the sinusoidal perturbation, i.e., $1/\gamma \ll \mathcal{T}$ or

$$\frac{\Omega}{\gamma} \ll 1. \tag{58}$$

These adiabatic assumptions, which are essential conditions for the two-state model [1], further simplify the map given by Eqs. (A7)–(A9) in the following way:

$$F_{n+1}=G^{(N)}(F_n), \tag{59}$$

$$p_{n+1}=e^{-\gamma\tau}p_n+\frac{1}{\gamma}[-V'(x_n)+A_0\cos(\Omega n\tau+\varphi)]\times\psi+(\gamma\tau)^{1/2}sF_{n+1}, \tag{60}$$

$$x_{n+1}=x_n+\frac{\psi}{\gamma}p_n+\frac{1}{\gamma}[-V'(x_n)+A_0\cos(\Omega n\tau+\varphi)]\left(\tau-\frac{1}{\gamma}\psi\right). \tag{61}$$

Notice that the consequence of the two assumptions is a direct replacement of $-V'(x_n)$ in the original QKP equations with $-V'(x_n)+A_0\cos(\Omega n\tau+\varphi)$ when a sinusoidal perturbation is considered. By imposing the overdamped limit, the momentum variable can be separated out, so that we are left with a two-dimensional map [see Eqs. (4) and (5)]:

$$F_{n+1}=G^{(N)}(F_n), \tag{62}$$

$$x_{n+1} = x_n + \left(\frac{\tau}{\gamma}\right)^{1/2} sF_n + \left(\frac{\tau}{\gamma}\right)[-V'(x_n) + A_0 \cos(\Omega n\tau + \varphi)]. \tag{63}$$

C. Two-state model of chaotic resonance from $G^{(2)}$ map

Consider a strongly damped particle moving in a bistable potential and subjected to chaotic fluctuations from a nonequilibrium heat bath. If the fluctuations were to arise from the class of even-order Tchebyscheff maps, we would expect the transition rate between the neighboring potential wells to be given by Eq. (45). Nevertheless, a more explicit transition rate expression is necessary for the purpose of theoretical analysis. This constraint has restricted our attention to fluctuations from the $G^{(2)}$ map, which give rise to the following escape rate:

$$K_r = \left\{1 + \left(\frac{\tau}{\gamma}\right)^{1/2} \int_{x_0}^{x_1} \left[\frac{V'(x)^2}{(kT)^{3/2}} - \frac{V''(x)}{(kT)^{1/2}}\right] dx\right\} \frac{\omega}{2\pi\gamma} e^{-\mu/kT}. \tag{64}$$

This escape rate, however, can be further simplified for a bistable potential since x_0 and x_1 are stationary points of the field so that the integral $\int_{x_0}^{x_1} V''(x)dx$ vanishes. The resulting rate

$$K_r = \left\{1 + \left(\frac{\tau}{\gamma}\right)^{1/2} \int_{x_0}^{x_1} \frac{V'(x)^2}{(kT)^{3/2}} dx\right\} \frac{\omega}{2\pi\gamma} e^{-\mu/kT}, \tag{65}$$

will be applied extensively in our subsequent analysis.

In the presence of an additional periodic force $A_0 \cos \Omega t$, Eqs. (62) and (63) with $\varphi = 0$ are the appropriate physical model of CR, if the adiabatic assumptions apply. Unlike the symmetric system considered for SR, or systems with asymmetry occurring in the bistable potential [30–32], our system contains asymmetry that comes from the statistical characteristics of the chaotic noise. This asymmetry appears in the escape rate as a perturbation to the prefactor of the Kramers rate, which is apparent in Eq. (65). To proceed with theoretical analysis, let us employ a simple analytical scheme developed by McNamara and Wiesenfeld [11]. This scheme is known as the two-state model and has been successfully applied to the analysis of SR.

To begin, let the two discrete states $-x_m$ and x_m represent the positions of the two potential wells of the bistable potential, while $P_-(t)$ and $P_+(t)$ are the probabilities that the system occupies these states at time t, respectively. In the presence of a weak periodic input signal $A_0 \cos \Omega t$, which biases the states $\pm$ alternately, the transition probabilities $W_-(t)$ and $W_+(t)$ out of the respective states $-x_m$ and x_m depend periodically on time. As a result, we can write the master equation for $P_+(t)$ as

$$\frac{dP_+(t)}{dt} = -W_- P_+ + W_+ P_-. \tag{66}$$

Then, by employing $P_+ + P_- = 1$, we arrive at

$$\frac{dP_+(t)}{dt} = -[W_+(t) + W_-(t)]P_+ + W_+. \tag{67}$$

The solution to Eq. (67) is given by

$$P_+(t|x_0,t_0) = g(t)\left[P_+(t_0) + \int_{t_0}^{t} W_+(\nu) g^{-1}(\nu) d\nu\right], \tag{68}$$

where

$$g(t) = e^{-\int_{t_0}^{t} [W_+(\nu) + W_-(\nu)] d\nu}. \tag{69}$$

In order to evaluate Eqs. (68) and (69), we need to first determine the transition probabilities $W_+(t)$ and $W_-(t)$. By noting that the potential

$$\hat{V}(x,t) = V(x) - A_0 x \cos \Omega t \tag{70}$$

varies with time adiabatically, we make the assumption that the escape rate is Eq. (65) with periodic modulation. More precisely, it has the form

$$W_+(t) = \left\{1 + \left(\frac{\tau}{\gamma}\right)^{1/2} \int_{-x_m}^{0} \frac{\hat{V}'(x,t)^2}{(kT)^{3/2}} dx\right\} \times \frac{\omega}{2\pi\gamma} e^{-\mu/kT} e^{A_0 x_m \cos \Omega t/kT}. \tag{71}$$

Let us next determine the integral within the prefactor of $W_+(t)$. We obtain

$$\begin{aligned}\int_{-x_m}^{0} \hat{V}'(x,t)^2 dx &= \int_{-x_m}^{0} [V'(x) - A_0 \cos \Omega t]^2 dx \\ &= \int_{-x_m}^{0} V'(x)^2 dx - 2A_0\mu \cos \Omega t \\ &\quad + A_0^2 x_m \cos^2 \Omega t,\end{aligned} \tag{72}$$

where μ is the height of the potential barrier between the two discrete states of the bistable potential. This evaluation leads to an expanded form of $W_+(t)$,

$$W_+(t) = \left\{1 + \left(\frac{\tau}{\gamma kT}\right)^{1/2} \left[\frac{1}{kT}\int_{-x_m}^{0} V'(x)^2 dx - \frac{2A_0\mu}{kT} \cos \Omega t + \frac{A_0^2 x_m}{kT} \cos^2 \Omega t\right]\right\} K e^{A_0 x_m \cos \Omega t/kT}, \tag{73}$$

with

$$K = \frac{\omega}{2\pi\gamma} e^{-\mu/kT} \tag{74}$$

being the classical Kramers escape rate in the strong friction regime. A similar evaluation shows that the transition rate $W_-(t)$ is given by

$$W_-(t) = \left\{1 - \left(\frac{\tau}{\gamma kT}\right)^{1/2} \left[\frac{1}{kT}\int_{0}^{x_m} V'(x)^2 dx + \frac{2A_0\mu}{kT} \cos \Omega t + \frac{A_0^2 x_m}{kT} \cos^2 \Omega t\right]\right\} K e^{-A_0 x_m \cos \Omega t/kT}. \tag{75}$$

Let us denote

$$\epsilon = \left(\frac{\tau}{\gamma}\right)^{1/2}. \tag{76}$$

Due to the symmetry of the bistable potential,

$$C = \frac{1}{(kT)^{3/2}}\int_{-x_m}^{0} V'(x)^2 dx = \frac{1}{(kT)^{3/2}}\int_{0}^{x_m} V'(x)^2 dx. \tag{77}$$

As τ/γ and A_0 are small quantities, we can simplify $W_+(t)$ and $W_-(t)$ by considering terms up to first-order in both τ/γ and A_0, i.e., ϵA_0:

$$W_+(t) = \left[1 + \epsilon C - \frac{2A_0\epsilon\mu}{(kT)^{3/2}}\cos\Omega t\right] K e^{A_0 x_m \cos \Omega t/kT}, \tag{78}$$

$$W_-(t) = \left[1 - \epsilon C - \frac{2A_0\epsilon\mu}{(kT)^{3/2}}\cos\Omega t\right] K e^{-A_0 x_m \cos \Omega t/kT}. \tag{79}$$

Substituting the expansion

$$e^{A_0 x_m \cos \Omega t/kT} = 1 + \frac{A_0 x_m}{kT}\cos\Omega t + \frac{1}{2}\left(\frac{A_0 x_m}{kT}\right)^2 \cos^2 \Omega t + \cdots \tag{80}$$

in Eqs. (78) and (79), we eventually obtain

$$W_+(t) = [1 + \epsilon C + (\epsilon\alpha + \eta)\cos\Omega t]K, \tag{81}$$

$$W_-(t) = [1 - \epsilon C + (\epsilon\alpha - \eta)\cos\Omega t]K, \tag{82}$$

where

$$\alpha = \frac{A_0 C x_m}{kT} - \frac{2A_0\mu}{(kT)^{3/2}}, \tag{83}$$

$$\eta = \frac{A_0 x_m}{kT}. \tag{84}$$

With Eqs. (81) and (82), we are able to determine the first-order probability distributions $P_+(t|x_0,t_0)$ and $P_-(t|x_0,t_0)$ (see Appendix B), which are given as follows:

$$\begin{aligned} P_+(t|x_0,t_0) = e^{-2K(t-t_0)}\Bigg\{ & \delta_K(x_0,x_m) - \frac{1}{2} - \frac{K\eta}{\sqrt{4K^2+\Omega^2}} \\ & \times\cos(\Omega t_0 - \phi) + \epsilon\Bigg[\frac{K\alpha}{\Omega}(\sin\Omega t - \sin\Omega t_0) \\ & \times[1 - 2\delta_K(x_0,x_m)] - \frac{1}{2}C\Bigg]\Bigg\} \\ & + \frac{1}{2} + \frac{K\eta}{\sqrt{4K^2+\Omega^2}}\cos(\Omega t - \phi) + \frac{1}{2}\epsilon C, \end{aligned} \tag{85}$$

$$\begin{aligned} P_-(t|x_0,t_0) = e^{-2K(t-t_0)}\Bigg\{ & \delta_K(x_0,-x_m) - \frac{1}{2} + \frac{K\eta}{\sqrt{4K^2+\Omega^2}} \\ & \times\cos(\Omega t_0 - \phi) + \epsilon\Bigg[\frac{K\alpha}{\Omega}(\sin\Omega t - \sin\Omega t_0) \\ & \times[1 - 2\delta_K(x_0,-x_m)] + \frac{1}{2}C\Bigg]\Bigg\} \\ & + \frac{1}{2} - \frac{K\eta}{\sqrt{4K^2+\Omega^2}}\cos(\Omega t - \phi) - \frac{1}{2}\epsilon C. \end{aligned} \tag{86}$$

Finally, in the asymptotic limit $t_0 \to -\infty$, Eqs. (85) and (86) become

$$\lim_{t_0\to-\infty} P_+(t) = \frac{1}{2} + \frac{K\eta}{\sqrt{4K^2+\Omega^2}}\cos(\Omega t - \phi) + \frac{1}{2}\epsilon C, \tag{87}$$

$$\lim_{t_0\to-\infty} P_-(t) = \frac{1}{2} - \frac{K\eta}{\sqrt{4K^2+\Omega^2}}\cos(\Omega t - \phi) - \frac{1}{2}\epsilon C. \tag{88}$$

With these results, we are ready to examine the time-varying mean of the particle

$$\begin{aligned} \langle x(t)|x_0,t_0\rangle &= \int xP(x,t|x_0,t_0)dx = \int x[P_+(t|x_0,t_0)\,\delta(x-x_m) \\ &\quad + P_-(t|x_0,t_0)\,\delta(x+x_m)]dx = x_m P_+(t|x_0,t_0) \\ &\quad - x_m P_-(t|x_0,t_0) = x_m[2P_+(t|x_0,t_0) - 1], \end{aligned} \tag{89}$$

where $\delta(\cdots)$ is the Dirac delta function. Taking the stationary limit $t_0 \to -\infty$ and employing Eq. (87), we obtain

$$\lim_{t_0\to-\infty}\langle x(t)|x_0,t_0\rangle = \frac{2K\eta x_m}{\sqrt{4K^2+\Omega^2}}\cos(\Omega t - \phi) + \epsilon C x_m, \tag{90}$$

showing that when $\epsilon = 0$, Eq. (90) reduces to the standard result of the white Gaussian noise. Thus, the effect of statistical asymmetry in the chaotic fluctuations is a constant positive bias in the time-varying mean, due to preferential transport of the particle to the positive state x_m.

Next, we shall determine the autocorrelation function of x, which is given by

$$\begin{aligned} \langle x(t+\nu)x(t)|x_0,t_0\rangle &= \int\int xyP(x,t+\nu|y,t)P(y,t|x_0,t_0)dxdy \\ &= \int\int xy[P_+(t+\nu|y,t)\,\delta(x-x_m) \\ &\quad + P_-(t+\nu|y,t)\,\delta(x+x_m)][P_+(t|x_0,t_0) \\ &\quad \times\delta(y-x_m) + P_-(t|x_0,t_0)\,\delta(y+x_m)]dxdy \\ &= x_m^2 P_+(t|x_0,t_0)[2P_+(t+\nu|x_m,t) - 1] \\ &\quad - x_m^2 P_-(t|x_0,t_0)[2P_+(t+\nu|-x_m,t) - 1]. \end{aligned} \tag{91}$$

To obtain the autocorrelation, it is necessary to consider terms up to ϵA_0^2 in Eqs. (81) and (82). By performing a detailed analysis as before to order ϵA_0^2, we arrive at the

following result after taking the asymptotic limit $t_0 \to -\infty$:

$$\lim_{t_0\to-\infty}\langle x(t+\nu)x(t)|x_0,t_0\rangle = x_m^2\Bigg\{e^{-2\kappa\nu} - \frac{4K^2\eta^2 e^{-2\kappa\nu}}{4\kappa^2+\Omega^2} \times\cos^2(\Omega t-\phi) + \frac{4K^2\eta^2}{4\kappa^2+\Omega^2} \times\cos(\Omega t-\phi)\cos[\Omega(t+\nu)-\phi] + \frac{K\eta^2 e^{-2\kappa\nu}}{4\Omega}[\sin 2\Omega t - \sin 2\Omega(t+\nu)] + \epsilon\Lambda\Bigg\}, \tag{92}$$

where

$$\Lambda = \frac{4K\eta C}{\sqrt{4\kappa^2+\Omega^2}}\Bigg\{\cos\frac{\Omega\nu}{2}\cos\left[\Omega\left(t+\frac{\nu}{2}\right)-\phi\right] - e^{-2\kappa\nu} \times\cos(\Omega t-\phi)\Bigg\} + \frac{2K\alpha e^{-2\kappa\nu}}{\Omega}[\sin\Omega t - \sin\Omega(t+\nu)] \tag{93}$$

and $\kappa = K(1+\eta^2/4)$. Interestingly, all the terms of order ϵA_0^2 have cancelled out.

The autocorrelation function is observed to depend on both $t+\nu$ and t even in the limit $t_0 \to -\infty$. As the phases $\theta = \Omega t - \phi$ are uniformly distributed between 0 and 2π from the point of view of real experimental measurement, it is reasonable to average $\lim_{t_0\to-\infty}\langle x(t+\nu)x(t)|x_0,t_0\rangle$ with respect to t over the entire forcing period $\mathcal{T}_\Omega = 2\pi/\Omega$ [1]. Representing this operation by the outer bracket $\langle\cdots\rangle$, we have

$$\langle\langle x(t+\nu)x(t)|x_0,t_0\rangle\rangle = \left(x_m^2 - \frac{2K^2\eta^2x_m^2}{4\kappa^2+\Omega^2}\right)e^{-2\kappa|\nu|} + \frac{2K^2\eta^2x_m^2}{4\kappa^2+\Omega^2}\cos\Omega\nu. \tag{94}$$

Equation (94) shows that the first-order effects of statistical asymmetry have been removed by the averaging operation because $(1/\mathcal{T}_\Omega)\int_0^{\mathcal{T}_\Omega}\Lambda dt = 0$.

The power spectral density $S(\hat{\omega})$ is the Fourier transform of $\langle\langle x(t+\nu)x(t)|x_0,t_0\rangle\rangle$. Thus,

$$S(\hat{\omega}) = \left(x_m^2 - \frac{2K^2\eta^2x_m^2}{4\kappa^2+\Omega^2}\right)\frac{4\kappa}{4\kappa^2+\hat{\omega}^2} + \frac{2\pi K^2\eta^2x_m^2}{4\kappa^2+\Omega^2}[\delta(\hat{\omega}-\Omega) + \delta(\hat{\omega}+\Omega)]. \tag{95}$$

Looking at the power spectral density, we observe that up to first order in ϵ, statistical asymmetry has not effected any change to the SNR when compared to SR. Quantitatively, we have

$$\mathrm{SNR} = \pi K\eta^2 + O(\epsilon^2), \tag{96}$$

where we have assumed x_m^2 to be more dominant than $2K^2\eta^2x_m^2/(4\kappa^2+\Omega^2)$ in the Lorentzian noise term. Equation (96) is the first-order SNR of CR due to $G^{(2)}$ map fluctuation. In fact, Eq. (96) continues to apply for fluctuation from the Ulam map by merely replacing ϵ by $-\epsilon$. In both cases, we observe a direct correspondence between CR and SR.

Finally, we would like to remark that this result provides theoretical insights into the seeming equivalence between chaotic and stochastic resonances that was observed by Ippen *et al.* through numerical simulations. In fact, if we were to consider fluctuations from the $G^{(3)}$ and $G^{(4)}$ maps, even faster convergence to SR would be expected. Thus, the correspondence between chaotic and stochastic resonances may apply to a larger class of chaotic fluctuations, rather than just the Ulam and the $G^{(2)}$ maps.

IV. SUMMARY AND CONCLUSIONS

We have analyzed the first-order effects of statistical asymmetry in even-order Tchebyscheff map fluctuations on a strongly damped particle moving in various potential fields. By solving the inhomogeneous Smoluchowski equation, we obtain the probability distribution of an ensemble of particles in a harmonic and bistable potential. Desymmetrization in the distribution is demonstrated both analytically and numerically as a result of statistical asymmetry. Based on our theoretical formalism, we have also determined an analytical expression for the prefactor of the escape rate over a potential barrier under the influence of statistically asymmetric noise. Our theory predicts that the effect of statistical asymmetry leads to an enhancement or suppression of Kramers escape rate, which is duly validated through numerical simulations. In addition, our analysis gives theoretical support to numerical evidence of chaotic resonance, and shows that chaotic resonance can directly correspond to stochastic resonance. Although our theoretical framework does not apply to the statistically symmetric odd-order Tchebyscheff maps, we have found through a simple symmetry analysis that their leading order effects correspond remarkably well with fluctuations that originate from white Gaussian noise.

ACKNOWLEDGMENTS

We would like to thank Dr. I. Goychuk, Professor Y.-C. Lai, Professor A. Pikovsky and Professor A. Dubkov for helpful and stimulating discussions. L.Y.C. is grateful to DSO National Laboratories for financial support.

APPENDIX A

This appendix shows the derivation of Eqs. (59)–(61). We begin by including a slow sinusoidal force to our chaotic kicked particle model as follows:

$$\frac{dp}{dt} = -\gamma p - \frac{\partial V(x)}{\partial x} + (\gamma m\tau)^{1/2}F^{\mathrm{I}}(t)\sum_n\delta(t-n\tau) + A_0\cos(\Omega t+\varphi). \tag{A1}$$

Restricting ourselves within the range $0^+ \leqslant t < \tau$ allows us to ignore the kicking force. As we have already determined the consequence of $V'(x)$, we will leave it out tentatively and will only put it back into the model at the end of the derivation. In this sense, we have

$$\frac{dp}{dt} + \gamma p = A_0 \cos(\Omega t + \varphi). \tag{A2}$$

Equation (A2) can be solved by integrating from $n\tau+0^+$ to $n\tau+t$. After some mathematical manipulation, we yield

$$p(n\tau+t) = e^{-\gamma t}p_n + \frac{A_0\gamma}{\gamma^2+\Omega^2}\{\cos[\Omega(n\tau+t)+\varphi] - e^{-\gamma t}\cos[\Omega n\tau+\varphi]\} + \frac{A_0\Omega}{\gamma^2+\Omega^2} \times\{\sin[\Omega(n\tau+t)+\varphi] - e^{-\gamma t}\sin[\Omega n\tau+\varphi]\}. \tag{A3}$$

This result enable us to evaluate the position of the particle. By integrating from $0^+ \leqslant t < \tau$ while employing Eq. (A3), we obtain

$$x(n\tau+t) = x_n + \frac{1}{\gamma m}(1-e^{-\gamma t})p_n + \frac{A_0}{m(\gamma^2+\Omega^2)} \times\left\{ \frac{\gamma\sin[\Omega(n\tau+t)+\varphi] - \Omega\cos[\Omega(n\tau+t)+\varphi]}{\Omega} - \frac{\gamma\sin[\Omega n\tau+\varphi] - \Omega\cos[\Omega n\tau+\varphi]}{\Omega} - \left(\frac{1-e^{-\gamma t}}{\gamma}\right) \times(\gamma\cos[\Omega n\tau+\varphi] + \Omega\sin[\Omega n\tau+\varphi])\right\}. \tag{A4}$$

Putting $t=\tau$, Eqs. (A3) and (A4) become

$$p_{n+1} = e^{-\gamma\tau}p_n + \frac{A_0\gamma}{\gamma^2+\Omega^2}\{\cos[\Omega(n+1)\tau+\varphi] - e^{-\gamma\tau}\cos[\Omega n\tau+\varphi]\} + \frac{A_0\Omega}{\gamma^2+\Omega^2}\{\sin[\Omega(n+1)\tau+\varphi] - e^{-\gamma\tau}\sin[\Omega n\tau+\varphi]\}, \tag{A5}$$

$$x_{n+1} = x_n + \frac{\psi}{\gamma m}p_n - \frac{A_0\psi}{m\gamma}\left\{\frac{\gamma}{\gamma^2+\Omega^2}\cos[\Omega n\tau+\varphi] + \frac{\Omega}{\gamma^2+\Omega^2}\sin[\Omega n\tau+\varphi]\right\} + \frac{A_0}{m\Omega}\frac{\gamma}{\gamma^2+\Omega^2} \times\{\sin[\Omega(n+1)\tau+\varphi] - \sin[\Omega n\tau+\varphi]\} + \frac{A_0}{m\Omega}\frac{\Omega}{\gamma^2+\Omega^2} \times\{-\cos[\Omega(n+1)\tau+\varphi] + \cos[\Omega n\tau+\varphi]\}, \tag{A6}$$

where $\psi=1-e^{-\gamma\tau}$. Equations (A5) and (A6) can be simplified further. In the meantime, by considering a strongly damped particle while reinserting the force field $V'(x)$ back into the equations leads to the following modified QKP map that includes the action of a slow temporal sinusoidal force

$$F_{n+1} = G^{(N)}(F_n), \tag{A7}$$

$$p_{n+1} = e^{-\gamma\tau}p_n - \frac{V'(x_n)}{\gamma}\psi + (\gamma\tau)^{1/2}sF_{n+1} + \frac{A_0}{\sqrt{\gamma^2+\Omega^2}}\cos[\Omega(n+1)\tau+\varphi-\delta] - \frac{A_0e^{-\gamma\tau}}{\sqrt{\gamma^2+\Omega^2}}\cos[\Omega n\tau+\varphi-\delta], \tag{A8}$$

$$x_{n+1} = x_n + \frac{\psi}{\gamma}p_n - \frac{V'(x_n)}{\gamma}\left(\tau - \frac{1}{\gamma}\psi\right) + \frac{2A_0}{\Omega\sqrt{\gamma^2+\Omega^2}}\sin\frac{\Omega\tau}{2}\cos\left[\Omega n\tau + \frac{\Omega\tau}{2} + \varphi - \delta\right] - \frac{A_0(1-e^{-\gamma\tau})}{\gamma\sqrt{\gamma^2+\Omega^2}}\cos[\Omega n\tau+\varphi-\delta], \tag{A9}$$

where $\delta=\arctan(\Omega/\gamma)$ and $m=1$ as before.

Finally, Eqs. (59)–(61) is attained by applying the adiabatic assumptions Eqs. (57) and (58) to the above QKP map, where we have combined φ and δ into a single phase since the former is arbitrary.

APPENDIX B

This appendix shows the derivation of Eqs. (85) and (86). Let us first employ Eqs. (81) and (82) to determine $g(t)$ of Eq. (69). Summing Eqs. (81) and (82), we have

$$W_+(t) + W_-(t) = (1+\epsilon\alpha\cos\Omega t)2K, \tag{B1}$$

which enables us to determine the integral:

$$\int_{t_0}^{t}[W_+(\nu) + W_-(\nu)]d\nu = 2K(t-t_0) + \frac{2\epsilon K\alpha}{\Omega} \times(\sin\Omega t - \sin\Omega t_0). \tag{B2}$$

This leads us to the following results for $g(t)$ and $g^{-1}(t)$:

$$g(t) = e^{-2K(t-t_0)}\left[1 - \frac{2\epsilon K\alpha}{\Omega}(\sin\Omega t - \sin\Omega t_0)\right], \tag{B3}$$

$$g^{-1}(t) = e^{2K(t-t_0)}\left[1 + \frac{2\epsilon K\alpha}{\Omega}(\sin\Omega t - \sin\Omega t_0)\right]. \tag{B4}$$

Then, we employ Eqs. (81) and (B4) to yield

$$\int_{t_0}^{t} W_+(\nu)g^{-1}(\nu)d\nu = \frac{K(\epsilon\alpha+\eta)}{\sqrt{4K^2+\Omega^2}}[e^{2K(t-t_0)}\cos(\Omega t-\phi) - \cos(\Omega t_0-\phi)] + \frac{2\epsilon K^2\alpha}{\Omega\sqrt{4K^2+\Omega^2}} \times [e^{2K(t-t_0)}\sin(\Omega t-\phi) - \sin(\Omega t_0-\phi)] + \left[\frac{1+\epsilon C}{2} - \frac{\epsilon K\alpha \sin\Omega t_0}{\Omega}\right] \times [e^{2K(t-t_0)}-1], \tag{B5}$$

where $\phi=\arctan(\Omega/2K)$. With Eq. (B3), we get

$$g(t)\int_{t_0}^{t} W_+(\nu)g^{-1}(\nu)d\nu = \frac{1}{2}+\frac{1}{2}\epsilon C + \frac{K\eta}{\sqrt{4K^2+\Omega^2}}\cos(\Omega t-\phi) + e^{-2K(t-t_0)}\left[-\frac{1}{2}-\frac{1}{2}\epsilon C - \frac{K\eta}{\sqrt{4K^2+\Omega^2}}\cos(\Omega t_0-\phi) - \frac{\epsilon K\alpha}{\Omega}\sin\Omega t_0 + \frac{\epsilon K\alpha}{\Omega}\sin\Omega t\right]. \tag{B6}$$

Putting these results with $P_+(t_0)=\delta_K(x_0,x_m)$ into Eq. (68) leads to Eq. (85). Moreover, because $P_+(t|x_0,t_0)+P_-(t|x_0,t_0)=1$, the corresponding result for $P_-(t|x_0,t_0)$, i.e., Eq. (86), ensues.

[1] L. Gammaitoni, P. Hänggi, P. Jung, and F. Marchesoni, Rev. Mod. Phys. **70**, 223 (1998).

[2] I. Goychuk and P. Hänggi, Phys. Rev. E **69**, 021104 (2004); Phys. Rev. Lett. **91**, 070601 (2003); T. Wellens, V. Shatokhin, and A. Buchleitner, Rep. Prog. Phys. **67**, 45 (2004); K. Park, Y.-C. Lai, Z. Liu, and A. Nachman, Phys. Lett. A **326**, 391 (2004); D. Babič, C. Schmitt, I. Poberaj, and C. Bechinger, Europhys. Lett. **67**, 158 (2004).

[3] P. Hänggi, ChemPhysChem **3**, 285 (2002); J. Dunkel, S. Hilbert, L. Schimansky-Geier, and P. Hänggi, Phys. Rev. E **69**, 056118 (2004); C.-H. Chang and T. Y. Tsong, *ibid.* **69**, 021914 (2004); J. A. Freund, L. Schimansky-Geier, B. Beisner, A. Neiman, D. F. Russell, T. Yakusheva, and F. Moss, J. Theor. Biol. **214**, 71 (2002).

[4] K.-P. Zeyer, A. F. Münster, and E. D. Gilles, Phys. Chem. Chem. Phys. **4**, 5988 (2002); Q. S. Li and R. Zhu, J. Chem. Phys. **115**, 6590 (2001).

[5] E. Ippen, J. Lindner, and W. L. Ditto, J. Stat. Phys. **70**, 437 (1993).

[6] A. Kovaleva and E. Simiu, in *Stochastic and Chaotic Dynamics in the Lakes: STOCHAOS*, edited by D. S. Broomhead, E. A. Luchinskaya, P. V. E. McClintock, and T. Mullin (American Institute of Physics, Melville, 2000), p. 428.

[7] R. Konnur, V. K. Jayaraman, and B. D. Kulkarni, Appl. Math. Lett. **13**, 69 (2000); A. Crisanti, M. Falcioni, G. Paladin, and A. Vulpiani, J. Phys. A **27**, L597 (1994).

[8] G. Nicolis, C. Nicolis, and D. McKernan, J. Stat. Phys. **70**, 125 (1993); E. Reibold, W. Just, J. Becker, and H. Benner, Phys. Rev. Lett. **78**, 3101 (1997).

[9] V. S. Anishchenko, A. B. Neiman, and M. A. Safanova, J. Stat. Phys. **70**, 185 (1993); T. L. Carroll and L. M. Pecora, Phys. Rev. Lett. **70**, 576 (1993); Phys. Rev. E **47**, 3941 (1993); S. Sinha and B. K. Chakrabarti, *ibid.* **58**, 8009 (1998); K. Arai, K. Yoshimura, and S. Mizutani, *ibid.* **65**, 015202(R) (2001).

[10] L. Y. Chew, C. Ting, and C. H. Lai, Phys. Rev. E **70**, 045203(R) (2004).

[11] B. McNamara and K. Wiesenfeld, Phys. Rev. A **39**, 4854 (1989).

[12] L. Y. Chew and C. Ting, Phys. Rev. E **69**, 031103 (2004).

[13] A. Hilgers and C. Beck, Phys. Rev. E **60**, 5385 (1999); C. Beck, Commun. Math. Phys. **130**, 51 (1990).

[14] H. Kantz, W. Just, N. Baba, K. Gelfert, and A. Riegert, Physica D **187**, 200 (2004).

[15] C. Beck, Physica A **169**, 324 (1990).

[16] H. Kantz and E. Olbrich, Physica A **253**, 105 (1998).

[17] A. Hilgers and C. Beck, Physica D **156**, 1 (2001); C. Beck, Nonlinearity **4**, 1131 (1991).

[18] C. Beck, Physica A **233**, 419 (1996).

[19] P. Hänggi, R. Bartussek, P. Talkner, and J. Łuczka, Europhys. Lett. **35**, 315 (1996); D. R. Chialvo, M. I. Dykman, and M. M. Millonas, Phys. Rev. Lett. **78**, 1605 (1997).

[20] P. Reimann, Phys. Rev. Lett. **86**, 4992 (2001).

[21] C. Beck, J. Stat. Phys. **79**, 875 (1995).

[22] H. Risken, *The Fokker-Planck Equation* (Springer-Verlag, Berlin, 1989).

[23] C. Nicolis and G. Nicolis, Phys. Rev. E **67**, 046211 (2003).

[24] W. Feller, *An Introduction to Probability Theory and its Applications* (Wiley, New York, 1971), Vol. II.

[25] H. A. Kramers, Physica (Amsterdam) **7**, 284 (1940).

[26] P. Hänggi, P. Talkner, and M. Borkovec, Rev. Mod. Phys. **62**, 251 (1990).

[27] P. Talkner, in *New Trends in Kramers' Reaction Rate Theory*, edited by P. Talkner and P. Hänggi (Kluwer Academic Publishers, Dordrecht, 1995), p. 47.

[28] A. Simon and A. Libchaber, Phys. Rev. Lett. **68**, 3375 (1992); C. Beck, Phys. Rev. E **49**, 3641 (1994); A. Hilgers and C. Beck, Europhys. Lett. **45**, 552 (1999).

[29] C. Beck, G. Roepstorff, and C. Schroer, Physica D **72**, 211 (1994).

[30] P. Jung and R. Bartussek, in *Fluctuations and Order: The New Synthesis*, edited by M. Millonas (Springer, New York, 1996), p. 35.

[31] R. Bartussek, P. Hänggi, and P. Jung, Phys. Rev. E **49**, 3930 (1994).

[32] A. R. Bulsara, M. E. Inchiosa, and L. Gammaitoni, Phys. Rev. Lett. **77**, 2162 (1996).